

On the Use of Low-Z Targets in Space-Based Hadron Calorimetry

O. Ganel, E.S. Seo, and J.Z. Wang

IPST, University of Maryland, College Park, MD 20742, USA

Abstract

In space-based experiments, detector mass is a critical concern. To allow an acceptable geometric acceptance, calorimeters used in such situations must be thin, and will thus not fully contain hadron showers. We discuss the benefits of using a low-Z target in front of thin calorimeters to force nuclear interactions and improve resolution. We report simulation results comparing several target options and a 'monolithic' configuration. The results demonstrate how calorimeter configuration, available mass, required energy resolution and 'good event' definitions can affect the optimal division of mass between the target and the calorimeter. Finally we suggest a method to optimize design choices based on the parameters of the experiment.

1 Introduction:

The driving concern in space-based high energy cosmic-ray experiments is collection power. The flux of particles requires large-area detectors with high acceptance to collect a sufficiently large data sample within an acceptable length of time. With a power-law spectrum falling roughly by a factor of 50 for every decade in particle energy above 1 GeV, experiments with a geometric factor (GF) on the order of $1 \text{ m}^2 \text{ sr}$ require three years to collect 10 protons above 10^{15} eV . The only practical way to measure a proton's energy above about 1 TeV is through ionization calorimetry, but calorimeters deep enough for nearly full containment of hadron showers are too massive to be incorporated into space-based experiments. A workable compromise is provided by thin calorimeters, but several issues must be addressed, as detailed below. A new generation of experiments, e.g., the balloon-borne Advanced Thin Ionization Calorimeter (ATIC) (Guzik et al., 1999), the Advanced Cosmic-ray Composition Experiment for the Space Station (ACCESS) (Israel et al., 1999) and the Cosmic Ray Energetics And Mass (CREAM) experiment (Seo et al., 1999), employing calorimeters with depths less than 2.5 nuclear interaction lengths (λ_{int}) are planned to fly during the coming decade. In this paper we discuss the process of optimizing the configuration of such experiments, including the incorporation of a target, choosing the target material, and dividing the stack thickness between target and calorimeter.

2 Thin Calorimetry:

A proton incident on a block of matter will interact inelastically after $1 \lambda_{\text{int}}$ on average, generating many secondary particles, mostly π^+ , π^- and π^0 in roughly equal proportions. The neutral pions decay almost immediately into pairs of photons, initiating electromagnetic (EM) cascades. A calorimeter must force at least one such interaction to provide an energy measurement. The energy of the resulting shower must then be measured with sufficient accuracy. The *effective* GF is thus the GF for particles in the detector's geometric acceptance that also interact sufficiently early to allow their energy to be measured reliably. The energy resolution of thin calorimeters, driven by leakage, is crude by the standards of ground-based devices, but sufficient for cosmic ray spectral measurements. For the purpose of reconstructing the rapidly falling spectra of various particles, it is more important to have energy independent resolution and response to hadron showers. This is achievable with thin calorimeters (Ganel et al., 1999a).

3 Space-Based Hadronic Calorimetry:

A space-based hadronic calorimeter should be deep enough in both λ_{int} and radiation lengths (X_0) to generate interactions and contain EM showers produced by secondary neutral pions, be light enough to fly, and yet retain an acceptable GF. At first glance, with limited mass one is tempted to use a monolithic device with

every gram exploited for the calorimeter. However, low-Z materials such as carbon generate more interactions for the same mass (in g/cm^2) compared to higher-Z materials, thereby providing improved resolution.

The mass limitation of space-based experiments implies that a configuration with a deep calorimeter and a thick target would be extremely limited in lateral extent and thus in collection power. The ATIC, ACCESS and CREAM baseline designs have proposed the use of $0.5 - 1.0 \lambda_{\text{int}}$ -thick low-Z (carbon) targets preceding a $20 - 27 X_0$ deep calorimeter as optimal.

4 Low-Z Targets and the Effective Geometry Factor:

Low-Z targets present a least-mass solution to the problem of forcing nuclear interactions. A $1 \lambda_{\text{int}}$ thickness of either a low-Z material (e.g. carbon) or high-Z material typically used in calorimeters (e.g. Fe, Pb, W, U, BGO, etc.) will provide similar interaction probabilities. However, the low-Z target will have a smaller λ_{int} value in g/cm^2 and will thus require less mass. This leaves a greater mass allowance for the calorimeter itself, allowing greater lateral size and increasing the effective GF. The lower target density increases the overall stack thickness, but the impact on the effective GF is much smaller. Another advantage of low-Z materials is the low ratio of λ_{int} to X_0 , which minimizes the dependence of calorimeter response on first-interaction depth.

4.1 Comparison of Low-Z Targets and a Monolithic Configuration: Balloon launch limits constrain payload masses to $1 - 2$ tons, with various support systems taking up about a third of the mass. A custom-written code was used to compare different target materials and a monolithic calorimeter option (calorimeter only, with no target) for balloon payloads. The combined calorimeter and target mass (calorimeter only, for the monolithic case) was set at 668 kg as the likely allowance to fit within the current 1000 kg mass limit of NASA's Ultra-Long Duration Balloon (ULDB) program. The calorimeter was assumed to be comprised of alternating layers of 3.5 mm tungsten and 0.5 mm scintillators, but the results of this study should apply to any high-Z calorimeter.

The target thickness was set at $0.5 \lambda_{\text{int}}$, corresponding to 19.1 cm, 14.4 cm, and 20.4 cm for carbon, alumina and beryllium, respectively. In the monolithic case one would be tempted to position the charge detector immediately atop the calorimeter, thereby maximizing the angular acceptance. Unfortunately, such a design would degrade data quality. Particles scattered back from the calorimeter would overlay the signal from the primary in the charge detector, making charge identification uncertain for protons at high energies (Ganel et al., 1999b). To avoid this, one must separate the charge detector vertically from the tungsten. The charge detector's lateral extent will then define the experiment's field of view. It is possible to make the charge detector very large, or to use a 'hat-like' design with active panels extending downwards to cover high-angle trajectories. This, however, would increase the mean incident angle, thereby reducing data quality by increasing atmospheric overburden (for balloon experiments), accepting more background events and degrading the tracking resolution. Such a design would also increase the size, cost and complexity of the charge detector, complicate the calorimeter readout, and make data interpretation much more difficult. To allow a fair comparison one must thus require comparable fields of view for the monolithic case and for the low-Z target cases.

The opening angle θ (see Fig. 1) of all targets was optimized for highest effective GF (35°). The same angle was assumed for the monolithic case to allow similar data quality. The calorimeter depth was similarly optimized. The calorimeter's lateral dimensions were set to fit the overall mass limit based on the opening angle and the target and calorimeter densities and thicknesses. Events were counted as good if the proton entered through the top of the target, interacted in the target or in the top of the calorimeter at least $20 X_0$

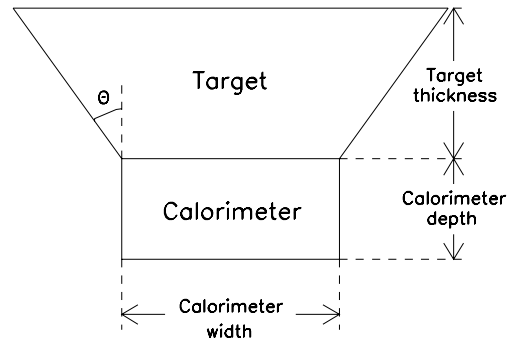


Figure 1: Schematic representing a space-based calorimeter preceded by an inverted trapezoidal target.

Table 1: Effective GF comparison for target options with target opening angles and calorimeter depth optimized, and calorimeter width set to fit in mass allowance.

Configuration	Calorimeter depth [cm]	Calorimeter width [cm]	Effective GF [m^2sr]
Carbon target	8.0	57.4	0.32
Alumina target	8.0	55.5	0.31
Beryllium target	8.0	58.5	0.33
Monolithic calorimeter	14.4	52.2	0.26

above its bottom and exited through the bottom or side of the calorimeter. The trajectory and first-interaction position were required to allow the shower development to have a vertical extent of at least $20 X_0$ from the first interaction to its point of exit from the calorimeter. This allows both sufficient containment of energy and track reconstruction. In the monolithic case the top-of-target requirement was substituted with a requirement that the proton pass through a charge detector positioned above a 19.1 cm air-gap, and defining the same 35° field of view as for the low-Z target cases.

From Table 1 we see that the three low-Z materials provide similar effective GF values. Of the three however, carbon is the most common, easiest to machine, and least toxic. Comparing the case of a carbon target to the monolithic case shows that the effective GF in the former case is about 25% higher. To achieve a comparable effective GF with the monolithic design requires the charge detector to be positioned with no air-gap, degrading the data quality and increasing cost and complexity, as described above. The conclusion from this study for a 1000 kg balloon payload is that a carbon target provides an optimal solution for cosmic-ray hadron calorimetry in terms of data quantity and quality, detector cost and complexity, and simplicity of data analysis. This conclusion would similarly apply to space-based calorimeters with mass limits of several tons.

4.2 Optimizing Calorimeter Depth vs. Target Thickness: Once a target material is selected, the target thickness can be optimized for greatest effective GF. Two trends compete in this process. On one hand, with thicker targets the interaction fraction for particles in the geometrical acceptance increases. On the other hand, the lateral extent possible with thicker targets is reduced, thereby limiting the geometrical acceptance.

The result of the optimization depends on the available mass, the definition of good events (determined by the required energy resolution) and on the target opening angle. To illustrate this dependence, the same custom-written code was used to optimize the calorimeter depth vs. carbon target thickness for a space-based BGO calorimeter. The total mass of calorimeter and target was set equal to the expected mass for the baseline ACCESS calorimeter (2730 kg). The total stack thickness was set to $2.4 \lambda_{\text{int}}$. Simulations using GEANT/FLUKA 3.21 (Brun et al., 1984; Arino et al., 1987) show that keeping this overall depth keeps the energy resolution, a measure of data quality, between $32\% \pm 1\%$ and $34\% \pm 1\%$. These overall (mass and thickness) parameters were kept constant to allow a fair comparison between all configurations. Thus, for each opening angle, as the BGO depth was varied from 30 cm to 50 cm, the carbon target thickness was varied from 39.4 cm to 4.7 cm, respectively, to complete the required $2.4 \lambda_{\text{int}}$ stack depth. The calorimeter lateral dimensions were determined by the materials and depths to meet the overall mass. Isotropically incident protons were simulated with random positions of incidence, interacting in the target or the top

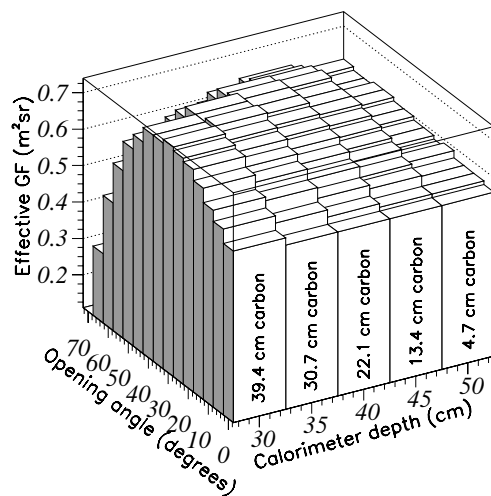


Figure 2: Effective GF as a function of target opening angle (θ) and BGO depth for simulated protons interacting at least 30 cm above the calorimeter bottom.

of the calorimeter (at least 30 cm above its bottom), and exiting through its bottom (see Fig. 1 for a schematic of such a configuration). Figure 2 shows the effective GF for ranges of opening angles and BGO depths. As can be seen, for the above parameters, the optimal values are a 30° opening angle and 30 cm BGO depth, or a 35° opening angle and 35 cm BGO depth, giving an effective GF of 0.74 m²sr. This is almost 28% higher than the best achievable with a 0° opening angle (0.58 m²sr). From Fig. 2 we see, however, that many combinations of BGO depth and target opening angle provide an effective GF close to the maximal value. For a BGO depth of 30 cm, for example, the target opening angle can be set between 15° and 45° while keeping the effective GF above 0.67 m²sr. Thus, if other considerations (e.g., charge detector power or cost per channel) constrain the design to targets with smaller opening angles, one could opt, for example, for a configuration with a 30 cm deep BGO calorimeter preceded by a 39.4 cm thick carbon target with a 15° opening angle, providing an effective GF of 0.69 m²sr. Configurations combining a thicker target (thinner calorimeter) and large opening angles (far left corner in Fig. 2) suffer greatly reduced effective GF as a result of too much mass being dedicated to the target. In such cases, the calorimeter width is so reduced that the effective GF shrinks. For thinner targets this effect is more limited, and the optimal opening angle slowly increases as BGO depth increases. If the required energy resolution allows, events can be accepted that interact deeper in the calorimeter. Simulations have shown that such a change increases the effective GF, shifting the optimal configuration to slightly smaller opening angle and calorimeter depth, and somewhat thicker target. A significant increase in payload mass will increase the effective GF and slightly increase the optimal target opening angle.

5 Discussion and Conclusions:

The optimal solution for a space-based hadron calorimeter is to employ a high-density calorimeter preceded by a carbon target. The target increases the effective GF by 25% compared to a monolithic configuration, for a comparable data quality. Shaping the target as an inverted truncated pyramid (Fig. 1) increases the effective GF by 28% or more, compared to a box-like target with lateral dimensions matching those of the calorimeter. The optimal configuration depends in a complicated way on the available mass and definition of acceptable event quality and energy resolution. To correctly optimize the design one must first determine the allowed mass and the data quality, i.e., energy resolution, required for the scientific goals of the experiment. Once these are known, one can determine the total stack depth, maximal depth of first interaction, minimal shower path-length, and number of tracking points required. Given these, the optimal design parameters and expected collection power can be determined with a relatively simple Monte Carlo program. Other constraints (e.g., charge detector size) also play a role when choosing among configurations with similar collection power. For the 2730 kg ACCESS baseline BGO calorimeter and carbon target combination with a required energy resolution of 30%–35%, the optimal configuration is a 30 cm deep calorimeter preceded by a 39.4 cm thick target with a 30° opening angle.

6 Acknowledgment:

This work was supported by NASA grant NAG5-5155.

References

- Arino, P.A. et al. 1987, FLUKA User's Guide, CERN, TIS-RP-190
- Brun, R. et al. 1984, GEANT User's Guide, CERN DD/EE/84-1
- Ganel, O. et al. 1999a, 26th ICRC , OG.4.6.01
- Ganel, O. et al. 1999b, STAIF-99 Space Tech. & Appl. Int. Forum AIP 1-56396-846-0/99, 272
- Guzik, T.G., et al. 1999, 26th ICRC , OG.4.1.03
- Israel, M.H., Streitmatter, R.E. and Swordy, S.P., STAIF-99 Space Tech. & Appl. Int. Forum AIP 1-56396-846-0/99, 114
- Seo, E.S. et al. 1999, 26th ICRC , OG.1.2.30